C II 158 μm observations of a sample of late-type galaxies from the Virgo cluster

K. J. Leech[1], H.J. Völk[2], I. Heinrichsen[1,2,4], H. Hippelein[3], L. Metcalfe[1], D. Pierini[2], C.C. Popescu[2,5], R.J. Tuffs[2], and C. Xu[4]

[1] ISO Data Centre, Astrophysics Division, ESA, Villafranca, Spain
[2] Max-Planck-Institut für Kernphysik, Saupfercheckweg 1, D-69117, Heidelberg, Germany
[3] Max-Planck-Institut für Astronomie, Koenigstuhl 17, D-69117, Heidelberg, Germany
[4] IPAC, Jet Propulsion Laboratory, Caltech 100-22, Pasadena, CA 91125, USA
[5] The Astronomical Institute of the Romanian Academy, Str. Cuţitul de Argint 5, 75212 Bucharest, Romania

Abstract. We have observed 19 quiescent Virgo cluster spiral galaxies with the Long Wavelength Spectrometer (LWS) onboard ESAs' Infrared Space Observatory (ISO), detecting 14 in the [CII] 157.741 μm fine structure line. Any influence of the Virgo cluster environment on the [CII] emission was found to be small compared with the strong dependence of the line emission on basic measurables such as morphology or bulk mass of the stellar component, as measured by the Near-IR (K$'$-band) luminosity. While the range of the [CII]-to-far-IR ratio is less than in other surveys, there is a good correlation between the strength of the [CII] line and the far-IR flux, as measured by IRAS. We find a trend of increasing [CII]-to-FIR flux ratio with increasing galaxy lateness. Moreover, the [CII]-to-K$'$-band flux ratio shows a two order of magnitude difference between RC3 type 0 and RC3 types later than 5. These two correlations express the relation between the mechanism of the [CII] emission and the massive star formation activity of the galaxy.

1 Introduction

The ISO (Kessler et al. [6]) Guaranteed Time programme VIRGO (Völk et al. *in prep*) is a photometric study of a complete volume-limited, unbiased sample of spiral, irregular and BCD galaxies from the Virgo cluster. Selecting galaxies from a cluster represents the most convenient way of ensuring completeness in a wide variety of intrinsic properties, embracing a large dynamic range in star-formation activity. In particular, the Virgo cluster was chosen for several reasons: the high level of completeness of the Virgo Cluster Catalogue (VCC) of Binggeli et al. [1], as described in Boselli et al. [2], to $B_T = 18$; at the distance to the cluster the typical angular sizes of the IR emitting regions are well matched to the angular resolution of ISO; and galaxies in the peripheral regions are thought to be freshly infalling from the field (Tully & Shaya [18]) and therefore less representative of the cluster environment.

While the VIRGO proposal is primarily photometric, we wished to observe many of these galaxies spectroscopically. Various constraints limited observations to the [CII] 157.741 μm cooling line, the most important gas cooling process in normal, i.e. non-starburst, late type galaxies, balancing the photoelectric heating from grains. It should probe photodissociation regions, e.g. Stacey et al. [16], associated with massive star formation, and also the diffuse components of the Interstellar Medium, e.g. Nakagawa et al. [11]. While in field galaxies the [CII] line has a luminosity of the order of 10^{-3} to 10^{-2} that of the total far-IR flux of a galaxy, e.g. Malhotra et al. [10], the Virgo sample galaxies are less active in star forming activity, even at the top end of the luminosity range observed.

At the distance of the Virgo cluster (taken to be 21 Mpc), the 70 arcsec diameter beam (Swinyard et al. [17]) of the LWS instrument (Clegg et al. [3]) covers an area of approximately 7 kpc in diameter. Optical images of the Virgo galaxies (Sandage et al. [14]) indicate that this will cover out to the observed spiral arms. In NGC 6946 the extended [CII] emission detected at this distance accounted for 70% of the total [CII] emission (Madden et al. [9]). Observation of Virgo galaxies with LWS will detect not only [CII] emission from the dense inner regions but, assuming Virgo galaxies are similar to NGC 6946, will primarily sample the [CII] emission from diffuse regions in and between the spiral arms.

This paper summarises the work of Leech et al. [7]. Pierini et al. [12] discusses the [CII] data and its relation to other measures of the star forming activity in more detail. Modelling of the relation between [CII] line emission and star formation history is deferred to Pierini et al. *in prep.*

2 Sample Selection and Observations

The criteria for selecting the VIRGO sample from the VCC are discussed in Leech et al. [7]. The 18 spirals selected are earlier than Scd, come from both the cluster core and periphery, and are complete to $B_T = 12.3$ mag. They provide a sample of relatively quiescent galaxies in comparison to other of spiral galaxy samples selected for ISO observations e.g. Malhotra et al. [10]. One other optically faint but IR bright core galaxy, VCC 1326, was observed to serve as a LWS/ISOPHOT cross-calibration target. Reference fields were also selected to check for foreground [CII] emission from the Milky Way.

The observing mode used was standard LWS grating range scans (AOT 2's) centred on the redshifted [CII] line. All observations reached the same sensitivity limit per wavelength point. Sets of observations were used to observe several galaxies in sequence, with one sky background position used for each set. The observations were made between 30^{th} June and 15^{th} July 1996 with no instrumental or satellite problems reported.

Information on these galaxies and the observing log are given in Leech et al. [7].

3 Data reduction and Results

The Auto Analysis Results from Off-Line Processing (OLP) version 7 were processed using the ISO Spectral Analysis Package (ISAP) version 1.6 by: discarding bad LWS data points; averaging scans for detector 8 (the one covering the 158 μm region); fitting the continuum; and finally fitting gaussians to any lines seen in the data to obtain flux and central wavelength.

Of the 19 galaxies observed, 14 were detected. Of the six background positions used, five had no detectable emission at galactic [CII] wavelengths and one was repointed to VCC 873, confirming the line flux and wavelength for that galaxy. In three galaxy observations (VCC 1110, 1326 and 1972) galactic [CII] emission was observed, and the data were fit with a line at the wavelength of galactic [CII] and one at the expected position of the Virgo [CII] emission.

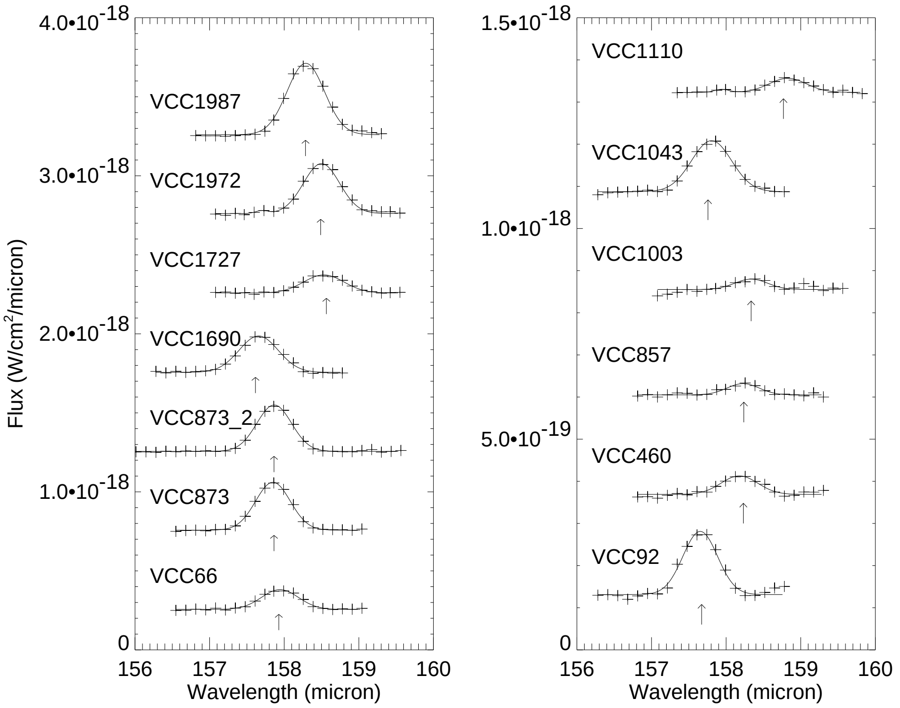

Examples of Virgo galaxy observations. The baselines are arbitrary. The expected positions of the [CII] emission lines from optical observations are marked by arrows. Datapoints are marked by a '+', with the vertical size indicating the size of the systemic error when larger than the symbol size. Lines are fit to the data.

Fig. 1.

The [CII] line spectral region for example galaxies are shown in Figure 1. In this Figure the baselines used during plotting are arbitrary. The continuum is quoted without subtracting any foreground emission from galactic emission. Note that the lines have not been resolved – linewidths are identical to the instrumental resolution (1100 km/s, Swinyard et al. [17]). Line fluxes, central wavelengths and continuum fluxes for all objects are given in Leech et al. [7].

4 Discussion

As already said in the Introduction, our sample of 19 VCC late type galaxies is biased toward low current star formation activity galaxies. In order to increase the range in current star formation activity, we add 5 low mass VCC galaxies observed by Smith & Madden [15].

4.1 The [CII] flux against far-IR flux

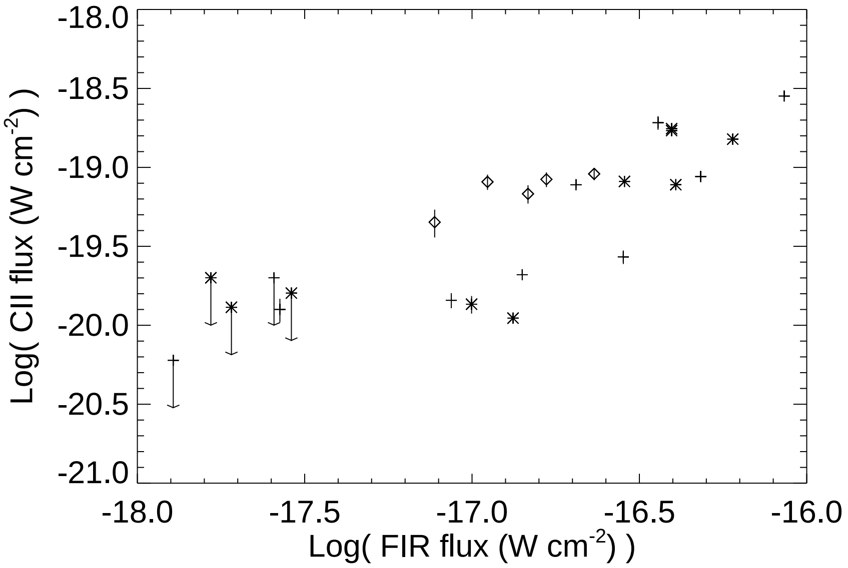

Fig. 2. [CII] flux against far-IR flux. Error bars are marked in the vertical, where they are larger than the symbol size, and upper limits are marked. Core galaxies are marked by '$*$', periphery by '$+$' and galaxies from Smith & Madden by diamonds.

Figure 2 shows the relation between the [CII] flux and the far-IR flux (from IRAS, $FIR = 1.26 \times 10^{-18}(2.58 \times F_\nu(60\mu m) + F_\nu(100\mu m))Wcm^{-2}$, Helou et al. [4]). Despite the spatial mis-match between the LWS 70 arcsec diameter circular aperture and the larger IRAS square apertures, there is a good correlation between these observed quantities within the approximately two orders of magnitude range in both quantities. We note that all the upper limits in the [CII] flux are found at the faint end of the far-IR emission.

When [CII] is detected, the [CII] to FIR ratio ranges from 0.1% to 0.5%. This covers the ranges expected for compact sources (0.2%), such as active star-forming regions, to the diffuse component on the ISM (0.6%) (Nakagawa et al. [11]). Galaxies observed by Stacey et al. [16] cover the range 0.15 – 0.6%, and in NGC 5713 the ratio is 0.7% (Lord et al. [8]).

4.2 Comparison with dust temperature

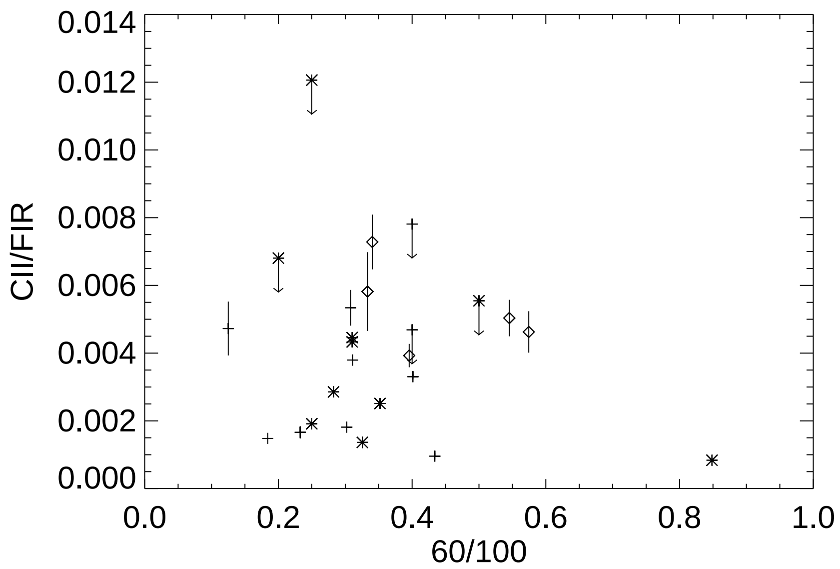

Fig. 3. [CII]/FIR ratio against dust temperature, indicated by 60/100 μm ratio. Error bars and upper limits are marked. Core galaxies are marked by '∗', periphery by '+' and galaxies from Smith & Madden by diamonds. VCC 1326 lies at the edge of this diagram with a 60/100 ratio of 0.85 but an apparently anomalously low [CII]/FIR ratio of 0.09%, and may be a starburst galaxy.

Figure 3 shows the [CII] to FIR ratio against the dust temperature, as measured by the ratio of the IRAS flux densities at 60 and 100 μm. The [CII]/FIR ratio is highest for galaxies with a 60 to 100 ratio of about 0.3 – 0.6, cf. Malhotra et al. [10].

4.3 [CII] and morphological type

Figure 4 shows the [CII]/FIR ratio against RC3 type. Ignoring the upper limits, there is marked difference between the ratio for RC3 types 0 – 3 against RC3 types later than 5. Galaxies with larger [CII]/FIR continuum ratios tend to have latter Hubble types.

If the [CII] flux is normalised by K′-band ($\lambda = 2.1\ \mu$m) flux, a measure of the number of old stars in the galaxy which constitute the bulk of the stellar mass component, c.f. Rix & Rieke [13], this difference with RC3 type is even more pronounced, as can be seen from Figure 5. This mass-normalization removes simple scaling effects in the relation between the [CII] and the K′-band luminosities (not shown).

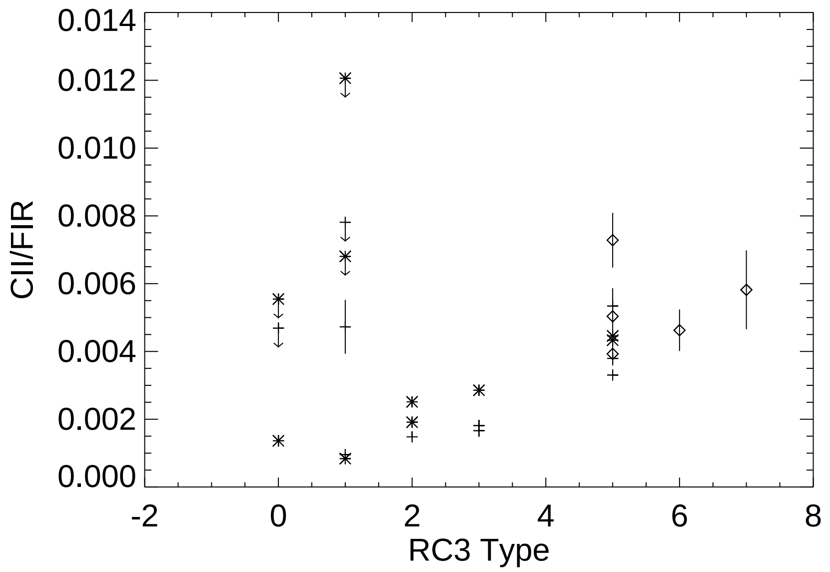

Fig. 4. [CII]/FIR ratio against RC3 Type. Error bars and upper limits are marked. Core galaxies are marked by '$*$', periphery by '+' and galaxies from Smith & Madden by diamonds.

Conversely, there is no apparent relation between the [CII] line properties and position in the cluster from Figures 2, 3, 4 and 5. Neither is there evidence for a relation between the [CII] line properties and disk HI mass surface density (within the LWS circular aperture), from Warmels [19], and therefore any relation of the [CII] emission to the diffuse HI component of the ISM is not obvious, at least for the central regions of the disks observed. This is interesting compared to the Madden et al. [9] results that find approximately

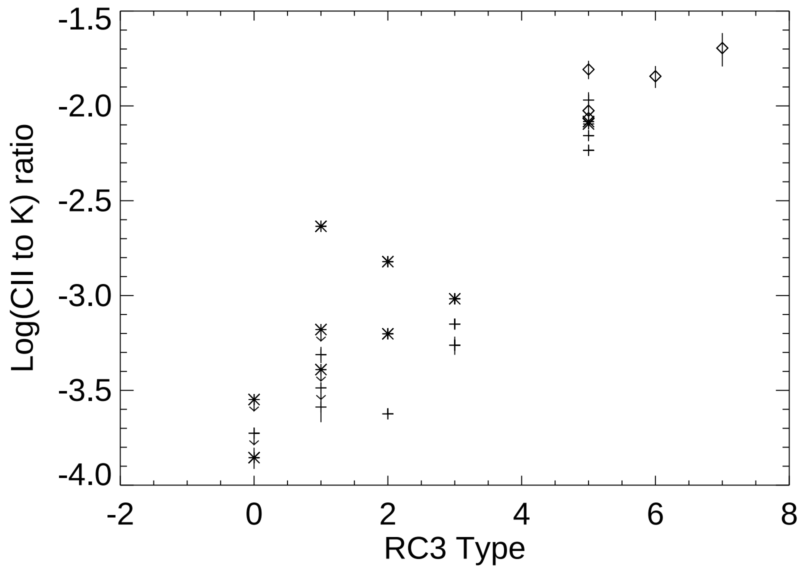

Fig. 5. [CII]/K$'$ flux ratio against RC3 Type. The difference between RC3 types 0 and 5 are more marked when the [CII] flux is normalised by a reliable estimate of the bulk of the galaxian stellar mass. Error bars and upper limits are marked. Core galaxies are marked by '$*$', periphery by '+' and galaxies from Smith & Madden by diamonds.

70% of the total [CII] emission from NGC 6946 arises from diffuse components of the disk. The lack of a [CII]–HI correlation integrated over the disks of the Virgo spirals therefore may come as a surprise. One potential explanation is that the central HI mass surface density is not well correlated to any global properties of the sample galaxies, e.g. the Hubble Type or the central molecular gas surface density (Pierini et al. *in prep*). However, we caution that we only have HI data for 12 galaxies and that larger samples are needed to establish firm trends in view of the large intrinsic scatter of the HI emission from galaxies of given morphological types.

5 Conclusion

We have detected the [CII] fine structure line in fourteen late-type Virgo cluster galaxies. A good correlation is found between the [CII] strength and the FIR flux. Moreover, we find evidence for a dependence of the [CII]-to-FIR flux ratio on the galaxy morphology, with the [CII]/FIR ratio increasing with later Hubble types. A stronger correlation with lateness is found for the

[CII]-to-K′-band flux ratio, the K′ flux representing the bulk of the stellar mass content of the galaxy.

Why is the [CII] to FIR ratio highest for galaxies with a 60/100 ratio of about 0.3 – 0.6, as shown in Figure 3, higher than for starburst galaxies? And why is there a marked difference in the [CII]/FIR ratio between RC3 types 0 – 3 and types later than 5? We interpret both these in the following way. Quiescent galaxies have a larger proportion of dust heating from the old low mass stellar population, which produces little or no UV and hence little [CII] line emission. On the other hand, starburst galaxies, produce copious hard-UV from their massive O stars which is very efficient at producing IR emission but is relatively inefficient at producing the [CII] line emission. Between these two extremes lie galaxies with a larger fraction of intermediate mass ($5 \leq$ M ≤ 20 $M_{\odot}$) stars that are efficient at both IR and [CII] line emission production from soft UV. Since massive star formation activity increases with increasing lateness, e.g. Kennicutt et al. [5], this lead to the correlation in the [CII]/FIR ratio against RC3 type plot, Figure 4. Note, however, that if the stars get too massive they become inefficient at producing the [CII] emission. This is discussed in more detail in Pierini et al. [12].

References

1. Binggeli B., Sandage A., Tamman G.A., 1985, AJ, 90, 1681
2. Boselli A., Tuffs R.J., Gavazzi G., Hippelein H., Pierini D., 1997, A&AS, 121, 507
3. Clegg P.E et al. , 1996, A&A, 315, L38
4. Helou G., Khan I.R., Malek L., Boehmer L., 1988, ApJS, 68, 151
5. Kennicutt R.C., Tamblyn P., Congdon C., 1994, ApJ, 435, 22
6. Kessler M.F. et al. , 1996, A&A, 315, L27
7. Leech, K.J. et al. , 1999, MNRAS, 310, 317.
8. Lord S.D. et al. , 1996, A&A, 315, L117
9. Madden S.C., Geis N., Genzel R., Herrmann F., Jackson J., Poglitsch A., Stacey G.J., Townes C.H., 1993, ApJ, 407, 579
10. Malhotra S., et al. , 1997, ApJ, 491, L27
11. Nakagawa T., et al. , 1998, ApJS, 115, 259
12. Pierini D., Leech K.J., Tuffs R.J., Völk, H.J, 1999, MNRAS, 303, L29
13. Rix H., Rieke M., 1993, ApJ, 418, 123
14. Sandage A., Binggeli B., Tammann G.A., 1985, AJ, 90, 395
15. Smith B.J., Madden S.C., 1997, AJ, 114, 138
16. Stacey G.J., Geis N., Genzel R., Lugten J.B., Poglitsch A., Sternberg A., Townes C.H., 1991, ApJ, 373, 423
17. Swinyard B., et al. 1998, In Proc. of SPIE Conference on Infrared Astronomical Instrumentation, Kona, Hawaii, SPIE Vol. 3354 pp 888-899
18. Tully R.B., Shaya E.J., 1984, ApJ, 281, 31
19. Warmels R.H., 1988, A&AS, 72, 427